Dual-Band and Wideband Self-Decoupled MIMO Antennas with Four Hybrid Modes

Wei Tang, *Student Member, IEEE*, Jiangwei Sui, *Member, IEEE*, Yan Wang, *Senior Member, IEEE*, Du Li, *Member, IEEE*, Junru Li, *Member, IEEE*, and Xiangwei Zhu, *Member, IEEE*

***Abstract*—A dual-band and wideband self-decoupled MIMO antenna design method using four hybrid modes is presented for mobile terminals. The perfect magnetic conductor (PMC) and perfect electric conductor (PEC) boundary conditions are utilized to analyze the four hybrid modes. It is found that by delicately optimizing the antenna geometry to make these four modes cancel out at two frequencies, self-decoupling can be achieved in the two bands simultaneously. Moreover, these four hybrid modes can be manipulated to be compatible with each other, so these two bands can be approached to achieve a wideband self-decoupling. Two demonstrational examples are designed to justify the proposed scheme. The results show that both the dual-band and wideband designs can achieve -10 dB impedance matching and 20 dB isolation across the desired bands, with the measured total efficiency higher than 71 %.**

***Index Terms*—Antenna decoupling, dual-band, hybrid modes, MIMO, mobile terminals, mutual coupling, wideband.**

I. Introduction

As A key technology of 5G/B5G communications, the multiple-input and multiple-output (MIMO) technique has been widely utilized in mobile terminals to improve channel capacity. And to provide more frequency resources, the 3.5 GHz (N78) and the 4.9 GHz (N79) bands, had been studied to be allocated as new 5G bands since 2015 [1], arousing the strong requirement for dual-band and wideband MIMO antenna system. However, severe electromagnetic coupling and interference between the antennas greatly deteriorate the system's performance [2].

To diminish the mutual coupling, various decoupling techniques have been proposed, such as using neutralization lines [3], [4], parasitic decoupling elements [5], lumped decoupling elements [6], special ground structures [7], [8] decoupling networks [9], [10], metasurface-based decoupling structures [11], and so on, where some of them can be well applied to the wideband [4], [7], and to the dual-band scenarios [8] – [11]. However, these decoupling structures all require to occupy extra precious space, which conflicts with the miniaturization requirement in mobile terminals.

To further minimize antennas' footprint, self-decoupling techniques not requiring extra decoupling circuits or structures have drawn great attention very recently, especially for mobile terminals. Firstly, two closely spaced antennas can be self-decoupled by arranging their geometries delicately [12], [13]. Besides, two antennas can be self-decoupled using orthogonal features, such as orthogonal modes [14], [15], orthogonal polarizations [16], and orthogonal patterns [17]. Another category of self-decoupling technique is based on the cancellation concept, such as coupling cancellation [18], [19], and mode cancellation [20], [21], which only deal with single-band decoupling. Moreover, in the existing cancellation-based works, only the S-parameters or input impedance of the antennas are studied, but the parameters of a more physical sense, such as the current mode, are not involved in exploring the physical mechanism.

In this letter, a self-decoupled scheme is proposed for dual-band and wideband MIMO antennas using four hybrid modes. Based on the mode cancellation scheme, the antenna is delicately designed to make the two corresponding modes at the low band cancel out with each other, and at the same time, the other two modes at the high band can also be mitigated simultaneously. Compared with the existing works, there are mainly two unique contributions of the proposed scheme:

1) it is the first time the same antenna topology can support both dual-band and wideband self-decoupling based on mode cancellation concept with corresponding dimension tuning;

2) the current mode for each excitation condition of even and odd modes is analyzed to reveal the physical mechanism behind the decoupling.

II. Working Mechanism

Fig. 1 illustrates the schematic diagram of the proposed self-decoupling method. In the low band, as shown in Fig. 1(a), the monopole and IFA modes are adopted, while the dipole and open slot modes are exploited in the high band, as depicted in Fig. 1(b). According to the even-odd mode theory [22], for the two-port symmetrical antenna structure shown in the left part of Figs. 1(a) and 1(b), the symmetrical plane is equivalent to an

Manuscript received xxxx xx, 2024; accepted xxxx. This work was supported in part by the National Key R&D Program of China under Grant 2021YFA0716500, in part by the National Natural Science Foundation of China under Grant 62201625, and in part by Guangdong Basic and Applied Basic Research Foundation under Grant 2021A1515110728. (*Corresponding author: Jiangwei Sui.*)

Wei Tang, Jiangwei Sui, Du Li, Junru Li, and Xiangwei Zhu are with the School of Electronics and Communication Engineering, Shenzhen Campus of Sun Yat-sen University, Shenzhen 518000, China (e-mail: tangw29@mail2.sysu.edu.cn; suijw@mail.sysu.edu.cn; lidu5@mail.sysu.edu.cn; lijr85@mail.sysu.edu.cn; zhuxw666@mail.sysu.edu.cn).

Yan Wang is with the Key Laboratory for Information Science of Electromagnetic Waves (MoE), School of Information Science and Technology, Fudan University, Shanghai 200433, China (e-mail: yanwang_fd@fudan.edu.cn).

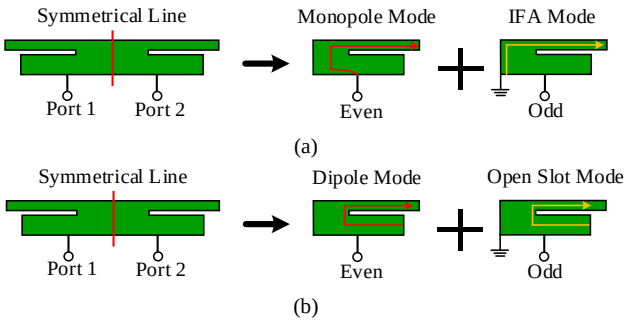

Fig. 1. Sketch diagram of the proposed self-decoupled scheme with four hybrid modes. (a) Modes description at the low band. (b) Modes description at the high band.

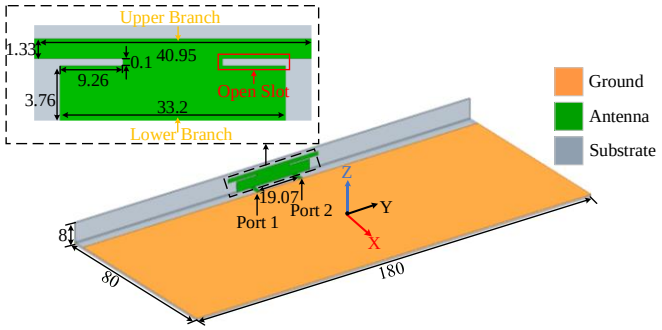

Fig. 2. Geometry of the mechanism-study two-port MIMO antennas. The unit used here is mm.

open-circuit condition (perfect magnetic conductor, PMC) for even mode excitations while it presents a short-circuit condition (perfect electric conductor, PEC) for odd mode excitations. The corresponding two-port S-parameters can be decomposed into two one-port antenna S-parameters under respective even mode and odd mode excitations as follows,

$$S_{11}(f)=\frac{S_{11\_even}(f)+S_{11\_odd}(f)}{2},\ f=f_1, f_2 \tag{1a}$$

$$S_{21}(f)=\frac{S_{11\_even}(f)-S_{11\_odd}(f)}{2},\ f=f_1, f_2, \tag{1b}$$

where $S_{11}(f)$ and $S_{21}(f)$ are the S-parameters of the two-port antennas on the left part of Fig. 1, $S_{11\_even}(f)$ and $S_{11\_odd}(f)$ are the S-parameters of the two one-port antenna systems on the right part of Fig. 1, and f_1 and f_2 are the center frequencies of the two desired bands. It is concluded from formula (1) that to make the S_{11} and S_{21} of the two-port antennas close to 0 to achieve perfect matching and decoupling, the two S-parameters of the one-port system in the right part of Fig. 1 both require to be close to 0, as illustrates in the following formula (2),

$$S_{11\_even}(f)\approx 0,\ f=f_1, f_2 \tag{2a}$$

$$S_{11\_odd}(f)\approx 0,\ f=f_1, f_2. \tag{2b}$$

It should be noted that formula (2) requires to be satisfied at f_1 and f_2 simultaneously to achieve dual-band or wideband self-decoupling. It is seen that the key point for mode cancellation is to make the two input impedances of these two pairs of modes close to each other at each band. Therefore, for the low band, the two modes are the λ/4 monopole mode and the IFA mode, which present similar current distributions and physical lengths, so it is of high potential that these two modes have similar input impedances. Similarly, for the same antenna geometry in the high band, the corresponding dipole mode and open slot mode are also probable to be canceled out with each other to achieve the eventual self-decoupling.

To prove these speculations, a mechanism-study example working in the N78 band (3.4 – 3.6 GHz) and N79 band (4.8 – 5 GHz) is shown in Fig. 2, where a two-port antenna system is symmetrically placed on a vertically-placed FR4 substrate whose permittivity is 4.4 and loss tangent is 0.02 with a dimension of 180 × 8 × 0.8 mm^3.

As is depicted in Fig. 3(a), in the EM simulation, the boundary condition of the symmetrical plane is set as the PEC for odd mode excitation with the other five boundary planes as the radiation condition, while PMC is set for the symmetrical plane under the even mode excitation. In this way, the two-port antenna pair turns into two one-port antenna systems, with the corresponding input impedance illustrated in the Smith chart in Fig. 3(b) for the PMC and PEC conditions, respectively.

For the 3.5 GHz, it is observed that the two input impedances, m_1 and m_3, are both very close to the original point of the Smith chart, meaning that the S_{11_even} (3.5) and S_{11_odd} (3.5) are both almost equal to 0 so that the matching and the decoupling have been simultaneously achieved at 3.5 GHz for the two-port antennas based on the formulas (1) and (2). At the same time, for the same antenna geometry, a similar phenomenon is observed for 4.9 GHz, as the marks m_2 and m_4 illustrate in Fig. 3(b). Therefore, benefiting from the comprehensive coordination of these four hybrid modes, the self-decoupling is achieved in the two bands simultaneously. To have a clearer justification, the S-parameters of the two-port antenna pair are presented in Fig. 4, which shows that the S_{11} and S_{21} at the two desired frequencies are all better than -25 dB, proving the obtained decoupling and matching of formula (1).

To study the physical mechanism, the current distributions of the one-port antenna under PEC and PMC conditions are shown in Fig. 5. As is shown in Figs. 5(a) and 5(b), in the low band, the current distribution of the even mode excitation is a typical monopole mode while it is of IFA mode for the odd mode excitation, coinciding well with those in Fig. 1(a). Similarly, in the high band, for the same antenna geometry, it is seen from Fig. 5(c) and Fig. 5(d) that it is of dipole mode under the even mode excitation and open-slot mode under the odd mode excitation, as expected in Fig. 1(b), and these two modes also share the similar input impedance.

III. Demonstration Examples

A. Dual-Band Self-Decoupled Antennas

To verify the generality of the proposed method, the above-studied dual-band MIMO antennas are placed 6.5-mm offset from the center line, as the geometry shown in Fig. 6.

To have a clearer insight, the evolution of the antenna is presented in Fig. 7. The antenna in Case 1 can achieve wideband decoupling higher than 10.5 dB, but it cannot support multi-band decoupling [20]. In Case 2, by adding two branches, dual-band decoupling is initially achieved. However, the area

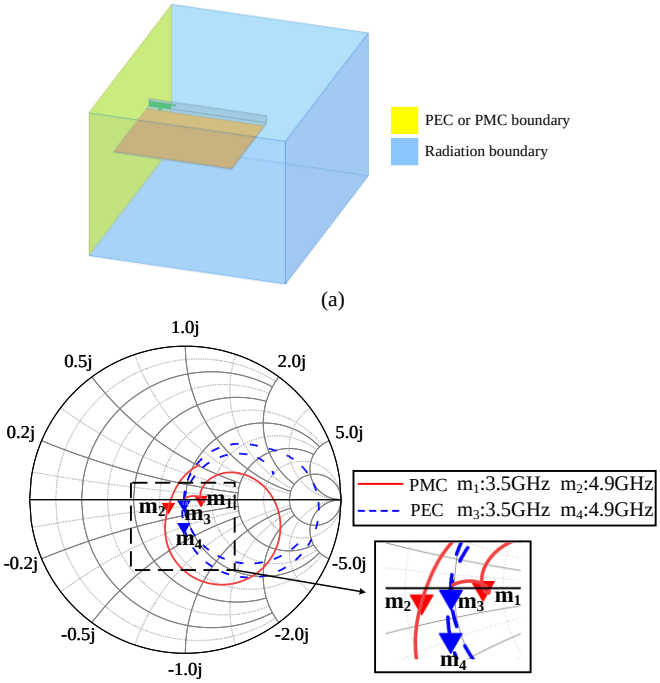

Fig. 3. Simulation model and the corresponding input impedances in Smith chart of the even mode and odd mode excitations. (a) Simulation model. (b) Input impedance.

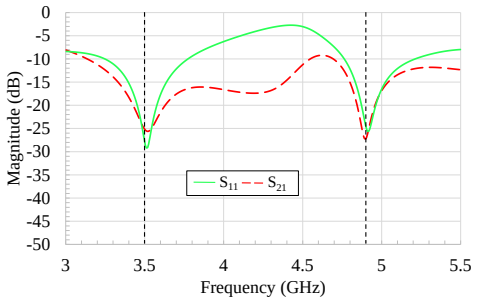

Fig. 4. Simulated S-parameters of the proposed two-port MIMO antennas.

between the two branches is not well utilized, so the antenna is not very compact. Case 3 merges the two branches into a symmetrically distributed one, achieving dual-band decoupling with a more compact and efficient design. Due to the different working modes for different bands, the dual-band decoupling can be independently tuned by adjusting the lengths of the upper branch and the slot.

The proposed antennas are then fabricated and measured. As shown in Fig. 8, the measured S-parameters agree well with the simulated ones. It is seen that the impedance matching is better than -10 dB in both the two bands. What's more, the isolations between the two ports are both better than 20 dB. This antenna can be used as a unit to form an eight-port antenna system by meandering the upper branch to lower the coupling between the two adjacent units, and the result is omitted here for brevity.

The total efficiency of the dual-band antennas is measured in an accredited near-field anechoic chamber. It can be found from Fig. 9 that the total efficiency in the low band varies from 81 % to 87 %, while that in the high band varies from 73 % to 89 %. After taking into hand's effect, the total efficiency will decrease to about 61 % and 54 % in the two bands, which is

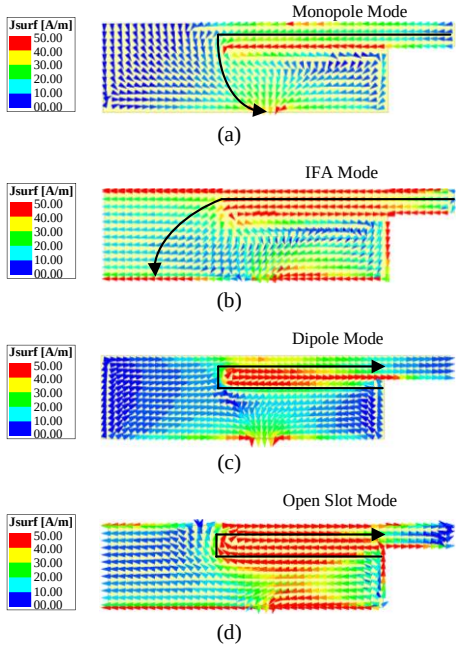

Fig. 5. Simulated current distributions of the one-port antennas. (a) Even mode at 3.5GHz. (b) Odd mode at 3.5GHz. (c) Even mode at 4.9 GHz. (d) Odd mode at 4.9 GHz.

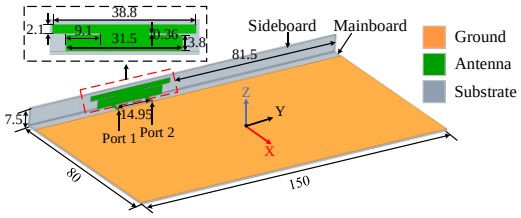

Fig. 6. Geometry of the proposed dual-band self-decoupled MIMO antennas. The unit used here is mm.

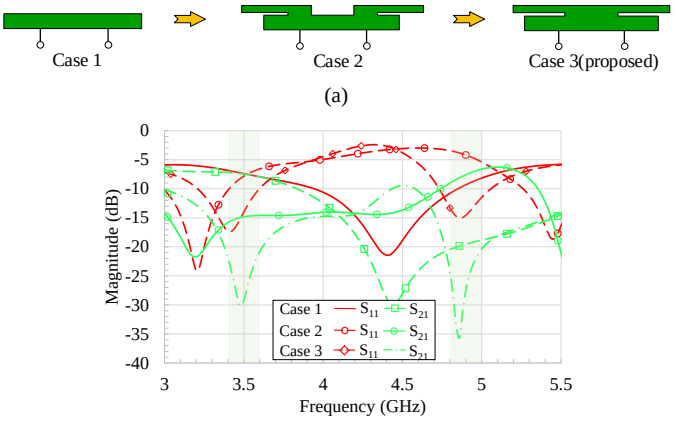

Fig. 7. The evolution of the proposed antenna. (a) Geometry. (b) S-parameters.

quite good for terminal antennas. Nowadays, maintaining a low specific absorption rate (SAR) has great significance for people's health. It can be seen in both the two bands, a low SAR is achieved, satisfying the requirement of lower than 2.0 W/kg.

To evaluate the diversity performance of the proposed MIMO antennas, the envelope correlation coefficient (ECC) is calculated, which is lower than 0.005 in both bands, showing a good MIMO spatial performance.

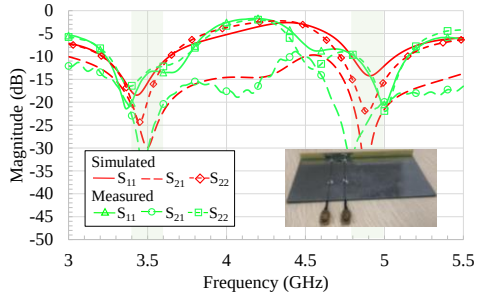

Fig. 8. Simulated and measured S-parameters of the proposed dual-band self-decoupled MIMO antennas.

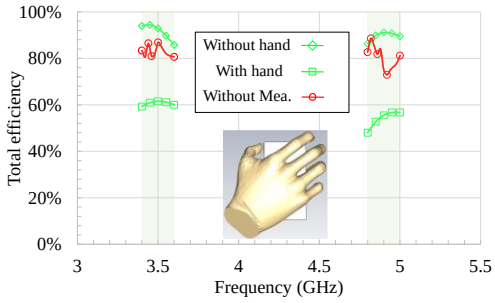

(a)

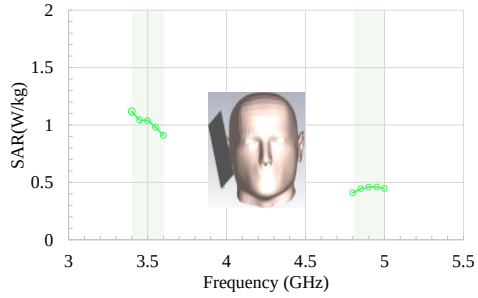

(b)

Fig. 9. Effect of the human body. (a) Total efficiency. (b) SAR.

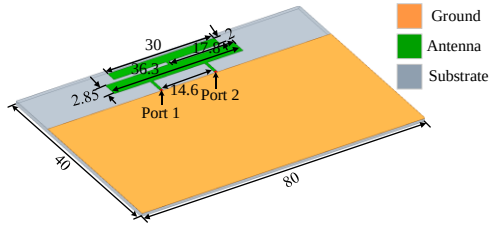

Fig. 10. Geometries of the proposed wideband self-decoupled MIMO antennas. The unit used here is mm.

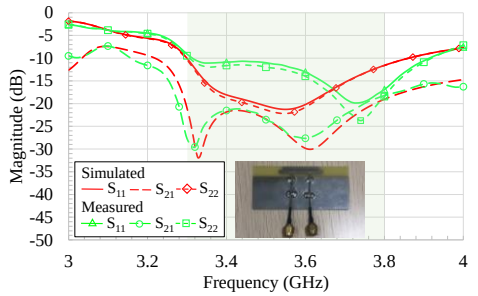

Fig. 11. Simulated and measured S-parameters of the proposed wideband self-decoupled MIMO antenna.

B. *Wideband Self-Decoupled Antennas*

To validate the generality of the decoupling scheme, the wideband antenna is constructed into a co-planar model with a detailed structure illustrated in Fig. 10.

As is observed for the S-parameter in Fig. 11, the matching condition is better than -10 dB in the wide N78 band from 3.3 to 3.8 GHz. Also, the isolation is better than -19 dB, showing good decoupling performance for the wideband scenario. A picture of the prototype is also inserted in Fig. 11. The radiation performance of the wideband antennas is also measured. It is found that across the wide N78 band, the measured total efficiency varies from 71 to 90 % with an average of about 82 %, and the ECC is lower than 0.042.

In summary, the results show that the four hybrid modes can coexist together as the two bands approach so that a wideband decoupling is successfully achieved.

TABLE I
Comparisons of Some Self-Decoupled MIMO Antenna Designs

Ref.	Frequency Band (GHz)	Impedance Matching	Isolation	Total Efficiency
[13][2019]	3.4 – 3.6 4.8 – 5.0	< -10 dB	> 17.5 dB > 20 dB	>50%
[15][2023]	3.3 – 3.6 4.4 – 5.0	< -6 dB	> 24 dB > 26 dB	> 71% > 68.3%
[20][2020]	3.3 – 4.2	< -6 dB	> 10.5 dB	63.1 – 85.1%
Proposed	3.4 – 3.6 4.8 – 5.0	< -10 dB	> 20 dB	81 – 87% 73 – 89%
	3.3 – 3.8	< -10 dB	> 20 dB	71 – 90%

C. *Discussions*

In this part, the proposed antennas are compared with some self-decoupled antennas recently reported from several aspects, as summarized in Table I. It is seen that the methods in [13] and [15] can support dual-band scenarios while that in [20] supports the wideband scenarios. On the contrary, the proposed scheme can be applied to both the dual-band and wideband scenarios, which benefits from the compatibility of the four hybrid modes. Although the cancellation of two modes is also used in [20], it only applies to the single-band scenario with -6 dB matching and -10 dB decoupling. Differently, a dual-band or wideband performance with -10 dB matching and -20 dB decoupling is obtained using the proposed self-decoupling scheme with four hybrid modes. Besides, the proposed designs prove higher efficiencies compared with the existing works for both the dual-band and wideband scenarios.

IV. Conclusion

In this letter, a dual-band and wideband self-decoupling scheme using four hybrid modes is proposed. Specifically, the proposed antennas present four different modes in the low band and high band for even and odd mode excitations. By designing the corresponding even and odd modes sharing a similar current distribution for the two bands simultaneously, a natural dual-band self-decoupling can be achieved. Moreover, these two bands can be approached to obtain a wideband decoupling. Taking into consideration the new principle and good performance, the proposed scheme provides a promising alternative for MIMO antenna designs in mobile terminals.

REFERENCES

[1] WRC-15 Press Release. (Nov. 27, 2015). World radiocommunication conference allocates spectrum for future innovation. [Online]. http://www.itu.int/net/pressoffice/press_releases/2015/56.aspx

[2] X. Chen, S. Zhang, and Q. Li, "A review of mutual coupling in MIMO systems," *IEEE Access*, vol. 6, pp. 24706–24719, 2018.

[3] A. Diallo, C. Luxey, P. L. Thuc, R. Staraj, and G. Kossiavas, "Study and reduction of the mutual coupling between two mobile phone PIFAs operating in the DCS1800 and UMTS bands," *IEEE Trans. Antennas Propag.*, vol. 54, no. 11, pp. 3063–3073, Nov. 2006.

[4] Y. Wang and Z. Du, "A wideband printed dual-antenna with three neutralization lines for mobile terminals," *IEEE Trans. Antennas Propag.*, vol. 62, no. 3, pp. 1495–1500, Mar. 2014.

[5] B. K. Lau and J. B. Andersen, "Simple and efficient decoupling of compact arrays with parasitic scatterers," *IEEE Trans. Antennas Propag.*, vol. 60, no. 2, pp. 464–472, Feb. 2012.

[6] C. Deng, D. Liu, and X. Lv, "Tightly arranged four-element MIMO antennas for 5G mobile terminals," *IEEE Trans. Antennas Propag.*, vol. 67, no. 10, pp. 6353–6361, Oct. 2019.

[7] J.-F. Li, Q.-X. Chu, and T.-G. Huang, "A compact wideband MIMO antenna with two novel bent slits," *IEEE Trans. Antennas Propag.*, vol. 60, no. 2, pp. 482-489, Feb. 2012.

[8] W. Zhang, Y. Li, K. Wei, and Z. Zhang, "Dual-band decoupling for two back-to-back PIFAs," *IEEE Trans. Antennas Propag.*, vol. 71, no. 3, pp. 2802–2807, Mar. 2023.

[9] J. Sui and K.-L. Wu, "A general T-stub circuit for decoupling of two dual-band antennas," *IEEE Trans. Microw. Theory Techn.*, vol. 65, no. 6, pp. 2111–2121, Jun. 2017.

[10] M. Li, Y. Zhang, D. Wu, K. L. Yeung, L. Jiang, and R. Murch, "Decoupling and matching network for dual-band MIMO antennas," *IEEE Trans. Antennas Propag.*, vol. 70, no. 3, pp. 1764–1775, Mar. 2022.

[11] F. Liu, J. Guo, L. Zhao, G. Huang, Y. Li, and Y. Yin, "Dual-band metasurface-based decoupling method for two closely packed dual-band antennas," *IEEE Trans. Antennas Propag.*, vol. 68, no. 1, pp. 552–557, Jan. 2020.

[12] K.-L. Wong, C.-Y. Tsai, and J.-Y. Lu, "Two asymmetrically mirrored gap-coupled loop antennas as a compact building block for eight-antenna MIMO array in the future smartphone," *IEEE Trans. Antennas Propag.*, vol. 65, no. 4, pp. 1765–1778, Apr. 2017.

[13] Z. Ren and A. Zhao, "Dual-band MIMO antenna with compact self-decoupled antenna pairs for 5G mobile applications," *IEEE Access*, vol. 7, pp. 82288-82296, 2019.

[14] A. Ren, Y. Liu, and C.-Y.-D. Sim, "A compact building block with two shared-aperture antennas for eight-antenna MIMO array in metal-rimmed smartphone," *IEEE Trans. Antennas Propag.*, vol. 67, no. 10, pp. 6430–6438, Oct. 2019.

[15] W. Hu et al., "Dual-band antenna pair with high isolation using multiple orthogonal modes for 5G smartphones," *IEEE Trans. Antennas Propag.*, vol. 71, no. 2, pp. 1949-1954, Feb. 2023.

[16] L. Chang, Y. Yu, K. Wei, and H. Wang, "Orthogonally polarized dual antenna pair with high isolation and balanced high performance for 5G MIMO smartphone," *IEEE Trans. Antennas Propag.*, vol. 68, no. 5, pp. 3487-3495, May. 2020.

[17] Y.-F. Cheng and K.-K. M. Cheng, "Decoupling of two-element printed-dipole antenna array by optimal meandering design," *IEEE Trans. Antennas Propag.*, vol. 68, no.11, pp.7328–7338, Nov. 2020.

[18] J. Sui and K.-L. Wu, "A self-decoupled antenna array using inductive and capacitive couplings cancellation," *IEEE Trans. Antennas Propag.*, vol. 68, no. 7, pp. 5289-5296, Jul. 2020.

[19] H. V. Singh, D. V. S. Prasad, and S. Tripathi, "Compact tightly-coupled self-decoupled MIMO antenna using internal hybrid tunning," *IEEE Trans. Circuits Syst. II, Exp. Briefs*, vol. 69, no. 12, pp. 4794–4798, Dec. 2022.

[20] L. Sun, Y. Li, Z. Zhang, and H. Wang, "Self-decoupled MIMO antenna pair with shared radiator for 5G smartphones," *IEEE Trans. Antennas Propag.*, vol. 68, no. 5, pp. 3423-3432, May 2020.

[21] A. Zhang, K. Wei, Y. Hu, and Q. Guan, "High-isolated coupling-grounded patch antenna pair with shared radiator for the application of 5G mobile terminals," *IEEE Trans. Antennas Propag.*, vol. 70, no. 9, pp. 7896-7904, Sep. 2022.

[22] D. M. Pozar, Microwave Engineering. Hoboken, NJ, USA: Wiley, pp. 328-331, 2012.